Silane Functionalization of Carbon Nanotubes (CNTs) and its Effects on the Properties of CNT/Epoxy Nanocomposites

Peng Cheng MA[1], Jang-Kyo KIM[1] and Ben Zhong TANG[2]
[1] Department of Mechanical Engineering and [2] Department of Chemistry, The Hong Kong University of Science & Technology, Clear Water Bay, Kowloon, Hong Kong, China

Keywords: *Carbon nanotubes (CNTs); Silane treatment; Epoxy based nanocomposites; Electrical properties; Fracture properties; Mechanical properties.*

Abstract

A new method is developed to chemically functionalize CNTs using a silane solution for polymer matrix composites. To oxidize and create active moieties on the CNT surface, the CNTs are exposed to UV light in an ozone environment, followed by reduction in lithium aluminum hydride and silanization using 3-glycidoxypropyltrimethoxy silane.

The effects of silane functionalization of CNTs on functional and mechanical properties of CNT/epoxy nanocomposites are evaluated. It was found that grafting silane molecules onto the CNT surface improved the CNT dispersion in the epoxy and enhanced the mechanical and thermal properties as well as fracture resistance of nanocomposites compared to those containing CNTs without functionalization. The electrical conductivity of nanocomposites decreased due to the wrapping of CNT with non-conductive silane molecules. The elemental analysis of CNT surface confirmed the presence silane functional groups that are reactive with polymer resin capable of forming covalent bonds.

1 Introduction

Possessing excellent strength, modulus, electrical and thermal conductivities along with a low density, carbon nanotubes (CNTs) have attracted much interest as the reinforcement for polymer matrix composites [1, 2]. CNT/polymer nanocomposites hold the promise of delivering exceptional mechanical properties and multi-functional characteristics. The potential of employing CNTs as reinforcement has, however, been severely limited because of the difficulties associated with dispersion of entangled CNTs during processing and the poor interfacial interactions between CNTs and polymer. To ensure effective reinforcements for polymer composites, proper dispersion and good interfacial adhesion have to be guaranteed [3].

Epoxy resin-based CNT nanocomposites have been extensively investigated in view of their potential applications in the electronics, aerospace and automotive industries [4]. However, there is no consensus regarding the efficiency of CNTs in improving the certain properties of nanocomposites [5-7]. These discrepancies probably arise from the large differences in the degree of entanglement and dispersion of CNTs in the resin, as well as in interfacial adhesion because the CNTs were not properly functionalized in many of the above studies [8].

This paper is part of a large project on the development of CNT functionalization techniques for improved dispersion and strong interfacial adhesion with polymer. In this paper, the effects of silane treatment are studied on various mechanical, fracture, and electrical properties of the CNT/epoxy nanocomposites.

2. Experiments

2.1 Materials and Composite Fabrication

CNTs used in this study were multi-walled carbon nanotubes (MWCNTs) whose diameter and length ranged between 10–20 nm and 10–50 μm, respectively. 3-Glycidoxypropyltrimethoxy silane (GPTMS) with 98% purity was used as the functionalization agent. The as-received CNTs were first purified via ultra-sonication in toluene as the dispersant. After drying, the purified CNTs were exposed to UV light in an ozone chamber to oxidize and create active moieties on the surface. This was followed by reduction in a lithium aluminum hydride solution and silanization in a GPTMS solution for 6 h at 60-65 °C [9].

The composites were made from epoxy, diglycidyl ether of bisphenol A (DGEBA), and a curing agent, m-phenylenediamine (mPDA). The functionalized CNTs were dispersed in ethanol for 1hr before adding the monomer epoxy, and the mixture was ultrasonicated for 1hr each at 60°C and 80°C, respectively.

The mixture was then outgassed at 80°C to eliminate entrapped air and the remaining ethanol. The mPDA hardener was added into the mixture in the ratio of 14.5/100 by weight. The composite was molded into a flat plate and cured at 80°C for 2hr, followed by post cure at 150°C for 2hr. Nanocomposites containing different weight fractions of untreated and silane-functionalized CNT were prepared [8].

2.2 Characterization and Mechanical Tests

Fourier transform infrared (FT-IR) spectrometry and field emission analytical transmission electron microscope (TEM) were used to characterize the changes in chemical structure and surface morphology of the CNTs before and after silane functionalization.

The storage modulus and tan δ were determined using a dynamic mechanical analyzer (DMA-7), according to the specification, ASTM Standard D4065. The glass transition temperatures, T_g, of nanocomposites were also determined from the maxima of the tan δ acquired from the DMA.

Three-point flexure test was performed to measure the mechanical properties of neat epoxy and nanocomposites according to the specification, ASTM Standard D790. Five specimens were tested for each set of conditions. Quasi-static fracture toughness of nanocomposites was measured using the compact tension test according to the ASTM Standard D5045. The test was performed on a universal testing machine at a cross-head 10mm/min. The maximum load, P_c, was recorded when the specimen was fractured, from which the stress intensity factor, K_{IC}, was calculated using the following equation:

$$K_{IC} = \frac{P_c}{b\sqrt{W}} \; f\left(\frac{a}{W}\right) \qquad (1)$$

Where

$$f\left(\frac{a}{W}\right) = \frac{\left(2+\frac{a}{W}\right)\left[0.886+4.64\left(\frac{a}{W}\right)-13.32\left(\frac{a}{W}\right)^2+14.72\left(\frac{a}{W}\right)^3-5.6\left(\frac{a}{W}\right)^4\right]}{\left(1-\frac{a}{W}\right)^{3/2}} \qquad (2)$$

W = 40mm and the specimen thickness b = 5mm.

A scanning electron microscope (SEM) was employed to exam the dispersion states of CNTs in the matrix and the fracture morphologies of the nanocomposites. The electrical conductivity of nanocomposites was measured at room temperature based on the four probe method using 10 mm square × 1 mm thick specimens on a resistivity/Hall measurement system.

3. Results and Discussion

3.1 Surface Functionalities of CNTs

Fig. 1 shows the FT-IR results of the CNTs before and after silane treatment. For the untreated-CNTs (Fig. 1A), the bands at 3419 and 1058 cm^{-1} are attributed to the presence of hydroxyl groups (-OH) on the surface of the MWCNTs, which are believed to result from either ambient atmospheric moisture bound to the MWCNTs or oxidation during purification of the raw material. Another band at 1626 cm^{-1} is assigned to the C=O stretching of quinone groups on the surface of CNTs.

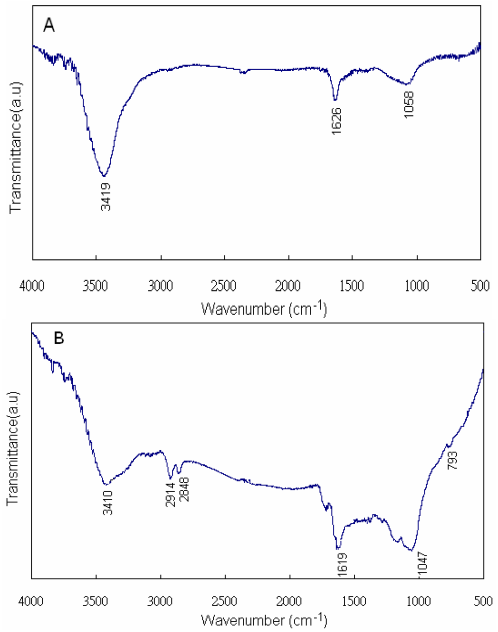

Fig. 1. FT-IR spectra of CNT (A: Untreated-CNT, B: Silane-CNT).

In the silane-CNTs (Fig. 1B), the band at 3410 cm^{-1} became broader and weaker, and two new bands at 2914 and 2848 cm^{-1} associated with the stretching of the methylene groups from the GPTMS molecules appeared. The weak signal at 793 cm^{-1} confirms the presence of the epoxy group on the GPTMS-modified MWCNTs. These results confirmed the attachment of silane molecules onto the CNT surface.

3.2 Dispersion and Surface Morphology of the MWCNTs

Fig. 2 shows the typical TEM images of the untreated-CNTs and silane-CNTs. The pristine CNTs were severely agglomerated (Fig. 2A). After the silane treatment, the agglomeration was significantly reduced (Fig. 2B). The individual CNTs were detached loosely without significant changes in their lengths. Some amorphous materials were attached to the end tips of the silane-treated MWCNTs (spot A in Fig. 2C). The detection of silicon by EDX (Fig. 2D) confirms that these amorphous materials were derived from the silane molecules. This observation further confirms that the surface layer of the CNTs has been activated by our method.

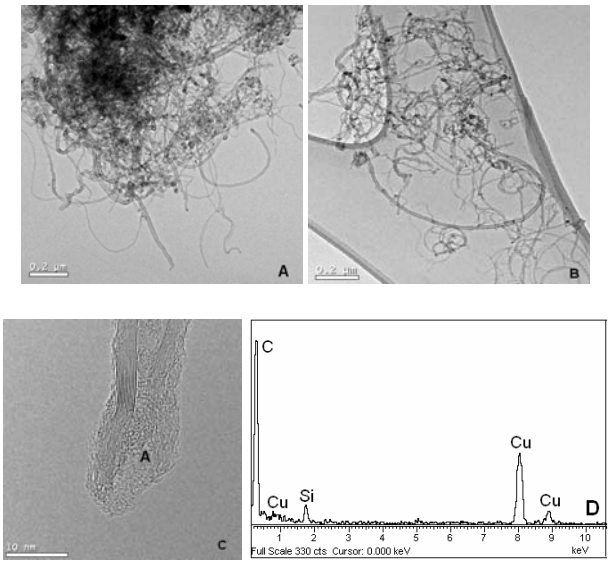

Fig. 2. Dispersion of CNTs (A: Untreated-CNT, B: Silane-CNT, C: End tips of Silane-CNT, D: EDX spectrum of spot A in C).

3.3 Dispersion of CNT in epoxy

Fig. 3 shows the SEM images of the fracture surface of nanocomposites, providing some insight into the CNT dispersion state. The untreated-CNT were present mainly in the form of agglomerates, whereas the silane-CNT were dispersed more uniformly, confirming much better dispersion of CNT in epoxy matrix. Improved interfacial interactions between the CNT and epoxy matrix were responsible. Silane molecules with epoxy end-groups were covalently attached on the CNT surface via the silanization reaction and partial hydrolysis of silane after functionalization [9], resulting in the conversion of CNT surface from hydrophobic to hydrophilic nature, and thus allowing the dispersion of silane-CNT in epoxy more uniform than the untreated-CNT.

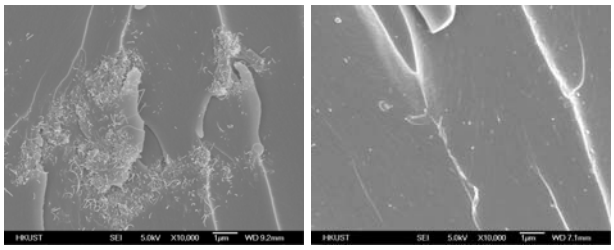

A: 0.25% untreated-CNT B: 0.25% silane-CNT

Fig. 3. SEM photographs of nanocomposite fracture surfaces showing the dispersion states of CNT.

3.4 Thermomechanical properties of nanocomposites

Fig. 4 shows the storage modulus and tan δ of nanocomposites obtained from the DMA analysis. The addition of silane-CNT to epoxy resin showed little influence on storage modulus in the glassy region. In contrast, there was a stronger effect of silane-CNT on storage modulus in the rubbery region at elevated temperatures where the improvement in the elastic properties of nanocomposites was clearly observed (Fig. 4a). This behavior can be explained in terms of interfacial interactions between the CNTs and epoxy. The improved interfacial interactions due to silane functionalization of CNT reduced the mobility of the local matrix material around the CNTs**,** increasing the thermal stability at elevated temperatures. There were marginal reductions in storage modulus of the nanocomposites containing untreated-CNT compared to the neat epoxy in the glassy region (Fig. 4c), as a result of CNT agglomeration. In the rubbery region, however, the storage modulus increased with increasing CNT loading, similar to the silane-CNT.

The tan δ values of the nanocomposites were calculated by dividing the loss modulus by the corresponding storage modulus obtained from the DMA analysis, as shown in Figures 4(b) and (d). It is interesting to note that the maximum value of tan δ for the neat epoxy was higher than those of the nanocomposites containing silane-CNT, while it was comparable to those of the nanocomposites containing untreated-CNT. Broad glass transition peaks and shoulders were noted from the tan δ curves of the nanocomposites containing silane-CNT (Curve B, C, and E in Fig. 4b). There are several possible reasons: i) the silane-treated CNT promoted the cross-linking reactions of epoxy and hardener,

effectively discouraging the movement of molecular chains; and ii) the covalent bonding between the silane-treated CNT and epoxy promoted energy dissipation from the matrix to the CNT, resulting in an increase in loss modulus.

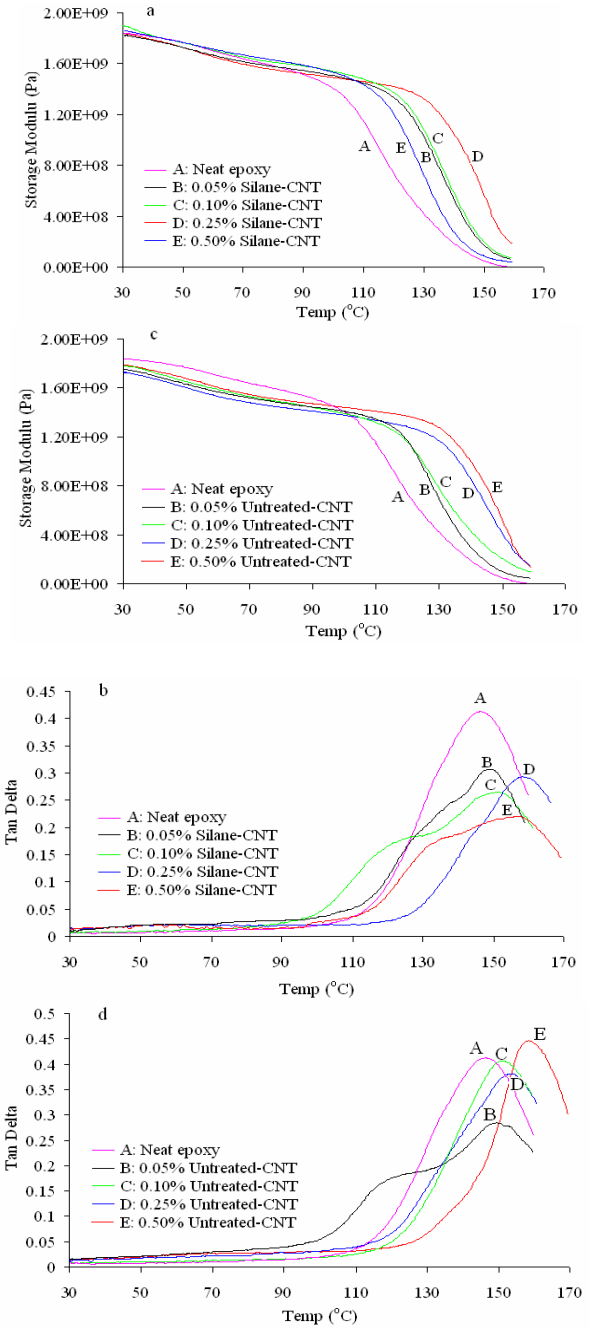

Fig. 4. Thermo-dynamic mechanical properties of nanocomposites.

From Figures 4(b) and (d), glass transition temperatures, T_g, were determined, which are shown as a function of CNT content in Fig. 5. The presence of CNT in the epoxy matrix increased the T_g of nanocomposites, with the effect being more pronounced for the silane-CNT. The difference in the extent of cross-linking reactions of epoxy was responsible for this observation: the silane-CNT can react with the m-PDA hardener more completely, introducing a higher cross-linking degree of the system than the untreated-CNT system. The epoxy functional groups are covalently attached onto the CNT after the silane treatment. Once the silane-CNT content exceeded a certain limit, say about 0.5 wt%, however, T_g started to decrease because the epoxy/diamine ratio exceeded the value required by the reaction stoichiometry, which in turn had a negative influence on the degree of cross-linking in the nanocomposites [8, 10].

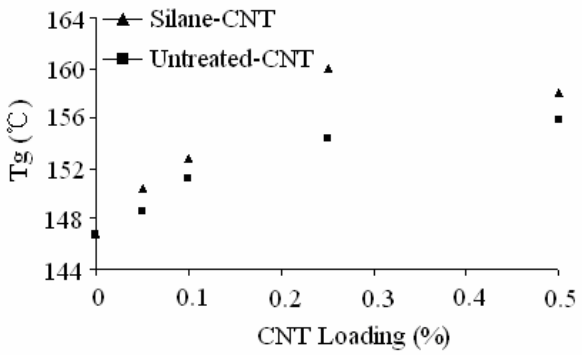

Fig. 5. Glass transition temperatures of nanocomposites as a function of CNT content.

3.5 Mechanical properties of nanocomposites

Fig. 6 shows the elastic moduli and strengths measured from the flexural test of nanocomposites, which are plotted as a function of CNT content. It is found that the modulus rapidly increased with increasing CNT content, before saturation at about 0.25 wt%. The nanocomposites containing silane-CNT exhibited a higher modulus than the untreated-CNT counterparts over the whole CNT contents studied. This result confirms the ameliorating effect of functionalization on the improvement of mechanical properties. The flexural strength of nanocomposites presented a similar trend: the strengths of the silane-CNT samples were consistently higher than the untreated-CNT counterparts when the reinforcement contents were 0.25 wt% or below. An anomaly was observed for the composite containing 0.5 wt% CNT with a reduction of flexural strength. It is suspected that the curing reaction between the DGEBA epoxy and amine hardener was adversely affected by the epoxy end-groups of the silane-CNT at this high CNT content.

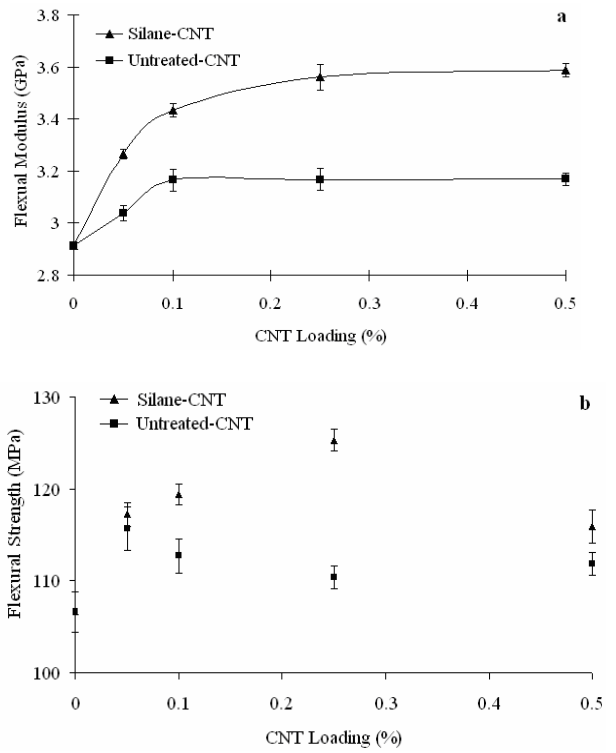

Fig. 6. Variations of (a) flexural modulus and (b) flexural strength of nanocomposites with CNT content.

3.6 Fracture resistance of nanocomposites

The quasi-static fracture toughness, K_{IC}, values of nanocomposites measured from the compact tension test is plotted as a function of CNT content in Fig. 7. It is interesting to note that the general trends of K_{IC} with respect to CNT content were different depending on whether the CNT was functionalized or not. The addition of untreated-CNTs into epoxy resulted in a continuous decrease of K_{IC}, whereas the nanocomposites containing silane-CNT showed a moderate increase in K_{IC}. These observations can be explained in terms of dispersion and interfacial interactions between the CNT and epoxy: for the untreated-CNT, both the dispersion in epoxy and the interfacial interaction were poor due to the agglomeration (Fig. 3A) and the inherently inert/hydrophobic nature of CNTs. After silane functionalization, both the dispersion of CNTs (Fig. 3B) and the interfacial interaction with epoxy were enhanced through the attachment of oxygen containing functional groups and silane molecules onto the CNT surface, as shown in our recent study [9].

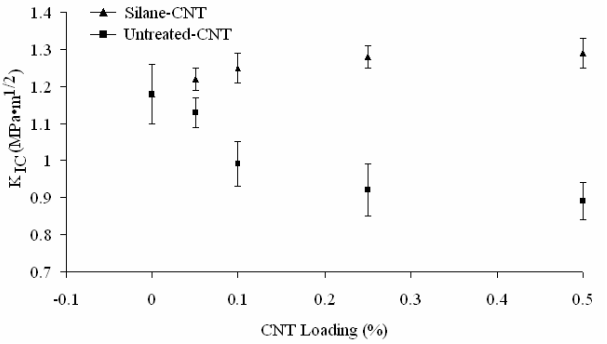

Fig. 7. Fracture toughness, K_{IC}, of nanocomposites with different CNT contents.

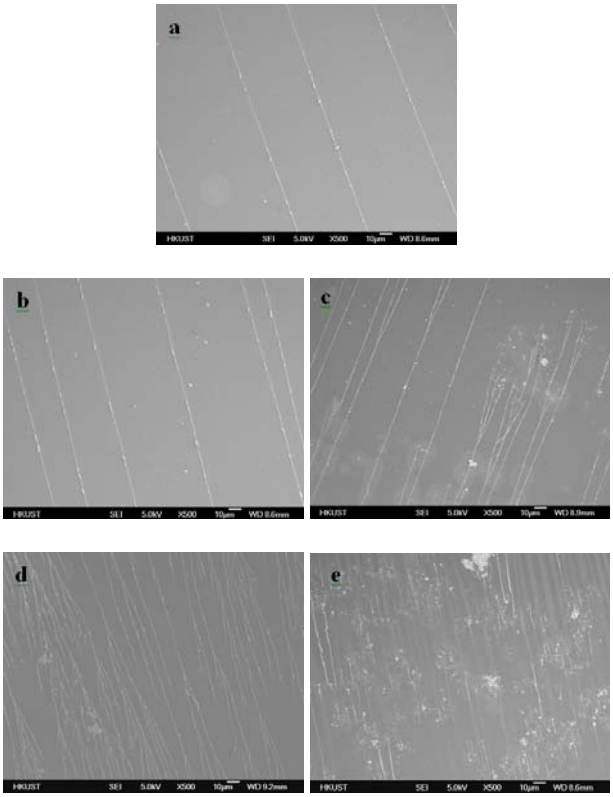

Fig. 8. Fracture surface morphologies of nanocomposites containing untreated-CNT: (a) neat epoxy; (b) 0.05 wt% CNT; (c) 0.1 wt% CNT; (d) 0.25 wt% CNT; and (e) 0.5 wt% CNT.

Major fracture mechanisms were identified based on the morphological analysis of the fracture surfaces of nanocomposites taken near the initial crack tip, as shown in Figures 8 and 9. The neat epoxy (Fig. 8a) exhibited a smooth, mirror-like fracture surface representing brittle failure of a homogeneous material. No obvious difference was observed between the neat epoxy and the composite containing 0.05 wt% untreated-CNT (Fig. 8b). With further increase in CNT content (Fig. 8c to e), the

CNTs tended to agglomerate into larger sizes, while the overall fracture surface morphology did not alter much with only marginal increases in the number of river markings. However, the corresponding fracture toughness consistently decreased because the CNT aggregates acted as the stress concentrators.

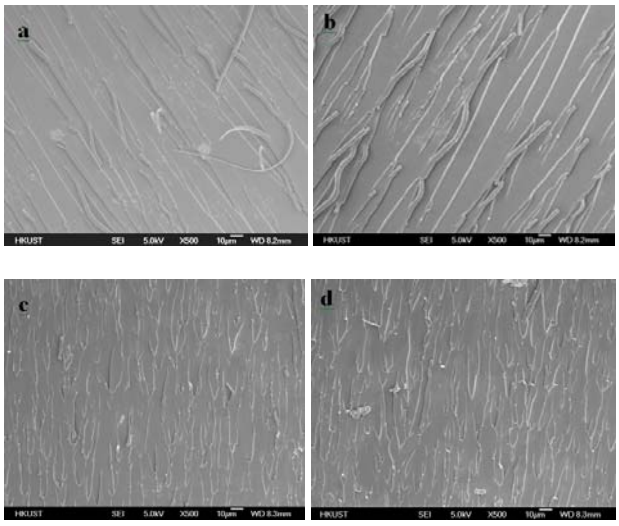

Fig. 9. Fracture surface morphologies of nanocomposites containing silane-CNT: (a) 0.05 wt% CNT; (b) 0.1 wt% CNT; (c) 0.25 wt% CNT; and (d) 0.5 wt% CNT.

In sharp contrast, the fracture surfaces for the composites containing silane-CNT revealed a systematic increase in the number of river marking and the corresponding surface roughness with increasing CNT content. At low CNT contents (0.05-0.1 wt%), there were straight and long river markings running parallel to the crack propagation direction (Fig. 9a and b). At higher CNT contents (0.25-0.5 wt%, Fig. 9c and d), these river markings became shorter and round-ended, similar to those observed in nanocomposites reinforced with high contents of nanoclay particles [11]. It appears that the increasing number of river markings roughly corresponds to the number of isolated, well-dispersed CNTs, which forced the cracks to propagate bypassing the CNTs and taking a long path. This resulted in dissipation of more energy through the well-known pinning and crack tip bifurcation mechanisms. However, the fracture toughness became more or less saturated at about 0.5 wt% CNT content, indicating that a higher CNT content would not result in further increase in fracture toughness because there is an increasing chance of agglomeration with increasing CNT content.

3.7 Electrical conductivity of nanocomposites

The aforementioned improvements in the thermo-mechanical, mechanical and fracture resistance of nanocomposites due to silane functionalization of CNT were at the expense of composite electrical conductivity. The electrical conductivity is plotted as a function of CNT content in Fig.10. The incorporation of the untreated-CNT increased the conductivity almost nine orders of magnitude, from 2.2×10^{-13} S/cm to 5.9×10^{-4} S/cm when the filler content was increased from 0.05 to 0.50 wt%. This observation was consistent with previous findings on CNT nanocomposites based on similar matrix materials [12, 13]. However, for the same filler content increase, the nanocomposites containing silane-CNT exhibited only a marginal - about two orders of magnitude - improvement in conductivity. The poor electrical conductivity of silane-CNT composites compared to the untreated-CNT counterpart was expected. There are two major reasons responsible for this observation. Firstly, the silane molecules with epoxy end-groups are covalently bonded to the CNT surface, which react with the amine hardener, leading to the wrapping of CNT by the epoxy after curing. The wrapping becomes more serious for well-dispersed individual CNTs. The wrapped polymer perturbs the π electron system of the CNT walls [14]. Secondly, the improved dispersion of CNTs in polymer matrix is known to be detrimental to the formation of electrical networks, especially at CNT contents above the percolation threshold. Further details of the correlation between the electrical conductivity and the dispersion states of CNT nanocomposites are presented elsewhere [15].

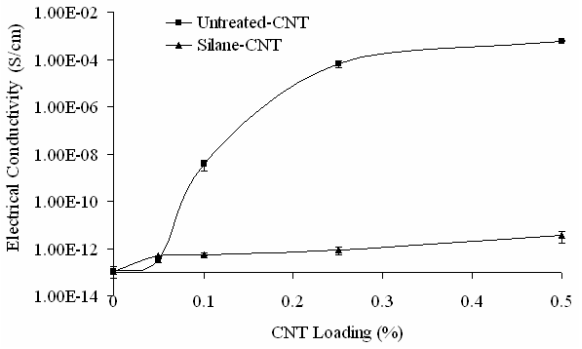

Fig. 10. Electrical conductivity of nanocomposites.

4. Conclusions

We developed a method for the chemical functionalization of the CNTs through silanization reaction. The hydrophobic surface of the MWCNTs was transferred to hydrophilic through silane

treatments. The results indicate good dispersion of CNTs in organic solvent and attachment of silane molecules on CNT surface. The effects of silane functionalization of CNT were investigated on the dispersion, mechanical and electrical properties of epoxy composites with different contents of CNTs. Major findings from this study are highlighted as following:

1. Grafting silane molecules onto the CNT surface can significantly improve the dispersion of CNTs in epoxy matrix.
2. Composites containing silane-CNT exhibited better flexural modulus and strength, fracture resistance than those containing untreated-CNTs.
3. The electrical conductivity of nanocomposites containing silane-CNT decreased due to the wrapping of non-conductive silane onto CNT surface and well-dispersed CNTs.
4. Above findings confirmed improved interfacial interactions due to covalent bonding between the silane functionalized CNTs and epoxy resin.

Acknowledgements

This project was supported by the Research Grant Council of Hong Kong SAR (Project No. 614505). Technical assistance from the Materials Characterization and Preparation Facilities (MCPF) of HKUST is appreciated.

References

[1] Thostenson E.T., Ren Z.F. and Chou T.W. "Advances in the science and technology of carbon nanotube and their composites: a review". *Comp Sci Tech,* Vol. 61, No. 1, pp 1899–912, 2001.

[2] Coleman J.N., Khan U. and Gunko Y.K. "Mechanical reinforcement of polymers using carbon nanotubes". *Adv Mater,* Vol. 18, No. 6, pp 689–706, 2006

[3] Fiedler B., Gojny F.H., Wichmann M.H.G., Nolte M.C.M. and Schulte K. "Fundamental aspects of nano-reinforced composites". *Comp Sci Tech,* Vol. 66, No. 16, pp 3115–25, 2006.

[4] Sun M.L. *"Application principle and theory of epoxy resins"*. 1st edition, China machine press (Beijing), pp 115–40, 2001.

[5] Zhu J., Peng H., Rodriguez-Macias F., Margrave J.L., Khabashesku V.N., Imam A.M., et al. "Reinforcing epoxy polymer composites through covalent integration of functionalized nanotubes". *Adv Funct Mater,* Vol. 14, No. 7, pp 643–48, 2004.

[6] Gojny F.H., Wichmann M.H.G., Kopke U., Fiedler B. and Schulte K. "Carbon nanotube-reinforced epoxy-composites: enhanced stiffness and fracture toughness at low nanotube content". *Comp Sci Tech,* Vol. 64, No. 15, pp 2363–71, 2004.

[7] Ajayan P.M., Schadler L.S., Giannaris C. and Rubio A. "Single-walled carbon nanotubes polymer composites: strength and weakness". *Adv Mater,* Vol. 12, No. 10, pp 750–53, 2000.

[8] Ma P.C., Kim J.K. and Tang B.Z.. "Effects of silane functionalization on the properties of carbon nanotube/epoxy nanocomposites". *Comp Sci Tech*, accepted, 2007.

[9] Ma P.C., Kim J.K. and Tang B.Z. "Functionalization of carbon nanotubes using a silane coupling agent". *Carbon,* Vol. 44, No. 15, pp 3232–38, 2006.

[10] Sandler J., Shaffer M.S.P., Prasse T., Bauhofer W., Schulte K. and Windle A.H. "Development of a dispersion process for carbon nanotubes in an epoxy matrix and the resulting electrical properties". *Polymer*, Vol. 40, No. 21, pp 5967–91, 1999.

[11] Siddiqui N.A., Woo R.S.C., Kim J.K., Leung C.C.K. and Munir A. "Mode I interlaminar fracture behavior and mechanical properties of CFRPs with nanoclay-filled epoxy matrix". *Comp Part A,* Vol. 38, No. 2, pp 449–60, 2007.

[12] Sandler J.K.W., Kirk J.E., Kinloch I.A., Shaffer M.S.P. and Windle A.H. "Ultra-low electrical percolation threshold in carbon-nanotube-epoxy composites". *Polymer,* Vol. 44, Np. 19, pp 5893–99, 2003.

[13] Martina C.A., Sandler J.K.W., Windle A.H., Schwarz M.K., Bauhofer W., Schulte K. and Shaffer M.S.P. "Electric field-induced aligned multi-wall carbon nanotube networks in epoxy composites". *Polymer*, Vol. 46, No. 3, pp 877–86, 2005.

[14] Grossiord N., Loos J., Regev O. and Koning C.E. **"**Toolbox for dispersing carbon nanotubes into polymers to get conductive nanocomposites". *Chem Mater,* Vol. 18, No. 5, pp 1089–99, 2006.

[15] Li J., Ma P.C., Chow W.S., To C.K., Tang B.Z. and Kim J.K. "Correlations between percolation threshold, dispersion state and aspect ratio of carbon nanotubes". *Adv Funct Mater*, in review, 2007.